

Feedback Control for a Small-Size Soccer Playing Humanoid Robot

Andrea Manni and Giovanni Indiveri
Dipartimento Ingegneria dell'Innovazione,
Università di Lecce

via per Monteroni, 73100 Lecce, Italy

Email: andrea.manni@unile.it and giovanni.indiveri@unile.it

Abstract— Given the intrinsic instability of walking humanoid robots, the design of controllers assuring robust stabilization of walking gaits is one of the most important goals.

Small humanoid robots today available in RoboCup, often lack computing power: they are frequently actuated by microcontroller based position servos with limited or no feedback. As a consequence it is very difficult to implement feedback control techniques on these platforms in order to guarantee stability. This paper describes a control architecture aiming at decoupling the problem of stable walking in the two relatively simpler problems of legs gait generation and upper body feedback control to guarantee dynamic stability. The presented implementation of the proposed architecture builds on the use of the GCoM point (Ground projection of the Center of Mass) that may be considered a suitable stability index only in quasi static robot states (like when kicking a ball from standing). The presented solution is particularly suited for small size robots having limited onboard computational power and limited sensor suits. The proposed method has been validated through Matlab[®] simulations and experimental tests performed on a Robovie-MS VStone's platform. Although the performed experiments are rather preliminary, they suggest that the designed architecture is effective.

Keywords: Control of Humanoid Robot, GCoM, Stability.

I. INTRODUCTION

Humanoid robots have always inspired the imagination of robotics researchers as well as the general public. Up until 2000, the design and construction of a humanoid robot was very expensive and limited to a few well funded research labs and companies (e.g., Honda Asimo [1] or Sony Qrio [2]). Starting in about 2001 advances in material sciences, motors, batteries, sensors, and the continuing increase in processing power available to embedded systems developers has led to a new generation of affordable small humanoid robots (by example, Pino [3]).

The creation of these humanoid robots also coincided with an increased interest in several high profile research oriented international robotics competitions (e.g., RoboCup [4]).

The Robot World Cup Soccer Games and Conferences (RoboCup) are a series of competition and events designed to promote the full integration of AI and robotics research. The robotic soccer provides a good test-bed for evaluation of various researches, e.g. artificial intelligence, robotics, image processing, system engineering, multiagent system.

The ultimate goal of the RoboCup initiative [4] is the following: *By mid-21st century, a team of fully autonomous*

humanoid robot soccer players shall win the soccer game, comply with the official rule of the FIFA, against the winner of the most recent World Cup.

Hence, the Humanoid league is essential for the initiative.

Guaranteeing dynamically stable walking gaits is one of the most important issues to be faced, but, given the present state of the art in RoboCup, its solution is technologically non trivial. Several methods have been presented in the literature to address the stability problem. Some of these are based on the inverted pendulum model for the bipeds [5], [6], [7]. Other techniques take directly into account dynamic stability indicators as the zero moment point (ZMP) [8], [9], [10] or the foot rotation indicator (FRI) [11].

The ZMP was originally introduced by Vukobratović [12], [13] and is defined as the point in the ground plane about which the total moments due to the ground contacts become zero in the plane. The FRI, introduced by Goswami [14], is defined as *the point on the foot/ground contact surface, within or outside the convex hull of the foot-support area, at which the resultant moment of the force/torque impressed on the foot is normal to the surface.*

This paper presents an overview on the actual state of the art in RoboCup and we propose a control law, building on Lyapunov Theory based nonlinear control methods, for the upper body joints able to guarantee quasi static walking stability of a small size and low-cost humanoid robot. The presented control architecture allows to decouple the gait generation issue and the overall stability of the system. The analysis of stability is addressed on the basis of the Ground projection of the Center of Mass (GCoM) and the support polygon. The remainder of the paper is organized as follows: an overview on RoboCup is presented in section II, the proposed control method is derived in section III. Simulation and experimental results are presented in section IV and, finally, conclusions are briefly discussed in section V.

II. AN OVERVIEW ON ROBOCUP: THE HUMANOID LEAGUE

To work towards the long-term goal of winning against the FIFA world champion, the RoboCup Federation added in 2002 a league for humanoid robots to their annual soccer championships. The progress made within this league since it was established is tremendous. For a detailed and up to date description of the state of the art the reader should refer

to the annual proceedings of the RoboCup Symposiums, the teams web pages and the RoboCup federation web page. The purpose of this section is to briefly and broadly report on the major trends in the area. The RoboCup Humanoid League competition rules [15] require the participating robots to have a human-like body plan. They consist of a trunk, two legs, two arms, and a head. The only allowed modes of locomotion are bipedal walking and running. The robots must be able to stand upright on their feet and to walk on their legs. The robots must be fully autonomous. No external power, computing power or remote control is allowed.

Because the humanoid robots have not been ready for playing soccer games so far, the robots had to demonstrate their capabilities by solving a number of subtasks. In the Penalty Kick competition two robots faced each other. While one robot tried to score a goal, the other defended. Each year, there is also a new technical challenge. In 2006, it consisted of a walking across rough terrain, dribbling around poles, and passing the ball between robots back and forth like reported in [15]. In 2005 and 2006, an autonomous 2 versus 2 match was also performed.

The teams which participated in the Humanoid League chose very different robot platforms. Most teams constructed their own robots, like Jaidee [16], Jupp [17], Robo-Erectus [18]. A few teams used expensive humanoid robots developed by the Japanese industry, e.g. Hoap-2 [19]. Some teams purchased servo driven commercial robots or robot kits, e.g. from Kondo [20] (e.g. [21], [22]), Vstone [23] (e.g. [24], [25]) or Robotis Inc. [26] (e.g. [27]).

The overall performance of the RoboCup humanoids is still far from perfect. Basic soccer skills, such as robust dynamic walking and kicking without loosing balance are not possessed by all robots. At present, in fact, in RoboCup although sensors are allowed and almost all robots have them, only few teams use them to control the robot stability with classical indexes (i.e. ZMP, FRI or GCoM) having limited onboard computational power.

The majority of kits used in RoboCup consist of sensomotoric actuators, a central processing unit, and several universal frame construction pieces. The upper torso contains the battery pack, the central processing unit, and a camera (some robots carry a PDA with a built-in camera). Most systems use smart, modular actuators that include a gear reducer, a precision DC motor and a control circuitry with networking functionality. The sensory feedback of the actuators includes the joint angle and the motor axis speed. Often, the supply voltage and the motor temperature are monitored for safety reasons. As for motion control tasks, sensory data from the tilt sensors are useful to detect different robot poses, especially if combined with the actuators angle values. This facilitates the decision of the appropriate stand up movements, once the robot has been overthrown by external forces.

III. CONTROL METHOD

The general control architecture of the proposed method has been presented in [28] and it is shown in figure 1 for the sake

of clarity. The method is kinematical in nature and relies on the assumption that the joint accelerations are small with respect to gravity. The basic idea is that the leg joints only are considered for locomotion planning while the upper body and arm joints are used for stabilization of the robot. This approach allows to decouple the gait generation and stabilization problems. This idea appears to be rather natural and indeed similar solutions had been already studied. By example in reference [29] the motion planning of a humanoid robot is decomposed into two parts, corresponding to the lower and upper body of the robot, to meet the collision-free and balance constraints respectively. Decoupling the gait planning and dynamic stabilization tasks is particularly important for small size robots that have limited computational power. In order for such decoupling to be effective, the cycle time of the stabilization controller needs to be suitably smaller than the gait period. Notice that this task division approach can be compared to [30] with the difference that in [30] the task division is implemented at an algorithmic level, while in the present case at a control architecture level.

With reference to figure (1) \ddot{q}_L , \dot{q}_L and q_L are the acceleration, velocity and position, respectively, of the leg joints. Likewise \ddot{q}_{UB} are the acceleration of the upper body joints, while \ddot{q}_R and q_R are the overall accelerations and positions, respectively, of the robot joints; v_t and r_t are the velocity and position of a target point in the ground plane to be used as reference value for a proper stability index as the ZMP, the FRI or the GCoM (Ground projection of the Center of Mass) that may be considered a suitable stability index only in quasi static robot states. Vectors \hat{q}_L and \hat{q}_{UB} are the estimates of the legs and upper body joint positions based upon the robots sensors; at last τ_L and τ_{UB} are the actuator leg torques and upper body torques. The gait generator block in figure (1) is a planner for the leg joints motions. The gait generator output is used to define the leg joint commands and it may use joint information also to perform obstacle avoidance planning or re-planning. As for the stability control, the direct kinematics model is used to compute the position of the center of the support polygon (i.e target point) as a function of the joint values.

The stabilization controller has as input the vector difference of the position of a target point inside the support polygon with the position of a proper stability index as the FRI (as reported in figure (1)), the ZMP or the GCoM in quasi static cases. The control objective of this control system is to drive the above defined error to zero by acting on the upper body degrees of freedom only. As discussed in the next section, in this paper we use GCoM as stability index because in the given application hypothesis it approximates FRI or ZMP that, by the way, are much more difficult to estimate as they depend also on joint accelerations and jerks.

A. Implementation issues

The stabilization feedback control loop described in figure (1) can be designed based upon a Lyapunov technique. Wanting the FRI point to converge on a target point r_t within the support polygon, a quadratic Lyapunov candidate function

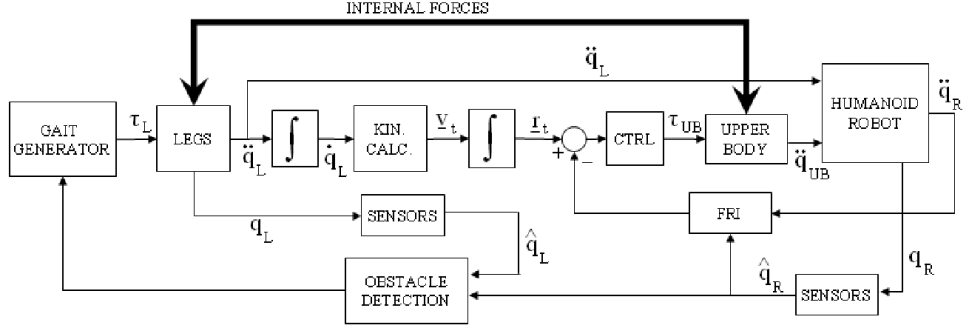


Fig. 1. Control architecture.

may be defined as:

$$V = \frac{1}{2} (\underline{r}_t - \underline{r}_{FRI})^T R (\underline{r}_t - \underline{r}_{FRI}) \quad (1)$$

where R will be a symmetric positive defined matrix, and \underline{r}_t and \underline{r}_{FRI} are the positions of a target point inside the support polygon and of the FRI respectively. Indicating with \underline{r}_{GCoM} the position of the ground projection of the center of mass, the following holds:

$$\underline{\delta} := \underline{r}_{FRI} - \underline{r}_{GCoM} \implies \lim_{a_i, \dot{\omega}_i \rightarrow 0} \underline{\delta} = \underline{0} \quad (2)$$

being a_i and $\dot{\omega}_i$ the linear and angular accelerations of each link. Notice that $\underline{\delta}$ is a continuous function of the link accelerations. Based upon the definition of FRI [14], it follows that if $|a_j| < g \forall j$, then $\|\underline{\delta}\|$ is upper bounded. If the support polygon is constant (i.e. either during a given single support phase or during a given double support phase), the time derivative of the candidate Lyapunov function (1) will be given by:

$$\begin{aligned} \dot{V} &= -\dot{\underline{r}}_{FRI}^T R (\underline{r}_t - \underline{r}_{FRI}) = \\ &= -(\dot{\underline{r}}_{GCoM} + \dot{\underline{\delta}})^T R (\underline{r}_t - \underline{r}_{FRI}) = \\ &= (\dot{q}_L^T J_L^T + \dot{q}_{UB}^T J_{UB}^T + \dot{\underline{\delta}}^T) R (\underline{r}_t - \underline{r}_{GCoM} - \underline{\delta}) \end{aligned} \quad (3)$$

being $\underline{\delta}$ defined in equation (2). Calling q_L, q_{UB} the legs and upper body joint variables and $J_L(q), J_{UB}(q)$ the legs and upper body Jacobian matrices such that

$$\dot{\underline{r}}_{GCoM} = J_L(q)\dot{q}_L + J_{UB}(q)\dot{q}_{UB}, \quad (4)$$

equation (3) suggests to compute the reference value of the upper joint velocities as

$$\dot{q}_{UBd} = J_{WUB}^\dagger \left[R (\underline{r}_t - \underline{r}_{GCoM}) - J_L \dot{q}_L + \dot{\underline{r}}_t \right] \quad (5)$$

being J_{WUB}^\dagger the weighted pseudo-inverse of matrix J_{UB} . In case J_{UB} should be full rank, J_{WUB}^\dagger results in $J_{WUB}^\dagger = W^{-1} J_{UB}^T (J_{UB} W^{-1} J_{UB}^T)^{-1}$ for some symmetric positive definite W of proper dimension. In case J_{UB} should be rank deficient in some pose, J_{WUB}^\dagger could be calculated on the basis of a singular value decomposition. Alternatively J_{WUB}^\dagger could

be taken to be a damped least squares inverse [31], hence avoiding singularity issues at the expense of control accuracy. Assuming $J_{WUB}^\dagger = W^{-1} J_{UB}^T (J_{UB} W^{-1} J_{UB}^T)^{-1}$, the extra degrees of freedom provided by the entries of the positive definite weight matrix W can be eventually dynamically assigned in order to try avoiding link collisions and kinematics singularities [31].

Notice that the use of the ground projection of the center of mass in place of the FRI in the control law makes \dot{V} equal to

$$\begin{aligned} \dot{V} &= -(\underline{r}_t - \underline{r}_{GCoM})^T R^T R (\underline{r}_t - \underline{r}_{GCoM}) + \\ &+ \underline{\delta}^T R \underline{\delta} - (\dot{\underline{\delta}}^T - \underline{\delta}^T R^T) R (\underline{r}_t - \underline{r}_{GCoM}) \end{aligned}$$

that is negative definite, thus guaranteeing the asymptotic stability of $(\underline{r}_t - \underline{r}_{FRI})$ (or, equivalently, of $(\underline{r}_t - \underline{r}_{GCoM})$) to zero, only in the limit of vanishing $\dot{\underline{\delta}}$ and $\underline{\delta}$. The use of \underline{r}_{GCoM} in place of \underline{r}_{FRI} makes the control law computationally much simpler as according to the FRI definition [14], $\dot{\underline{r}}_{FRI}$ will depend on the joint accelerations and jerks. Moreover simulations (here not reported for the sake of brevity) have confirmed that for the joint accelerations of interest on the considered platform, $\underline{\delta}$ and $\dot{\underline{\delta}}$ are indeed negligible.

As for the q_L, \dot{q}_L and $\dot{\underline{r}}_t$ in the upper body joint control law (5), notice that q_L and \dot{q}_L are known as they are generated by the legs gait controller and $\dot{\underline{r}}_t$ is generated in such a way that \underline{r}_t is always within the support polygon. Generally $\dot{\underline{r}}_t$ is designed such that during the single support phase \underline{r}_t moves within the support polygon in the same direction of the walking gait so that at the end of the single support phase, when the support polygon becomes the one of the double support phase, \underline{r}_t will be located approximately in its center.

It should be noticed that the above described motion control law does not take into account effects related to the motion of the foot on the ground that, during the single support phase, is assumed to be still. Indeed effects as jiggling, stumbling or slipping may have a relevant impact on the overall stability of the robot. These effects could be considered within the very same architecture if the FRI or ZMP were directly measured using force and torque sensors mounted on the feet. Yet this solution is technologically rather complex to be realized on

small size platforms and, for the time being, was not explored.

IV. SIMULATION AND EXPERIMENTAL RESULTS

The presented control approach has been validated both in simulation and experimentally. The simulations have been performed in Matlab using the Robotics Toolbox realized by P. I. Corke [32]. These simulations were intended to validate the proposed approach on a purely geometrical and kinematical level rather than on a dynamic one. To this extent, the single support phase of the humanoid robot was modeled as an open kinematics chain with a fixed base (i.e. the support polygon). The performed simulations were purely kinematical and did not include any dynamic effect. As for a dynamic validation, no simulation has been realized, but rather experimental tests have been performed. These tests are rather preliminary as the control law was not processed on the humanoid's onboard CPU, but on an external computer connected to the robot via serial link. Moreover only the sagittal plane joint velocities \dot{q}_{UB} were assigned according to equation (5) whereas the dorsal and transverse plane joints were controlled in open loop.

In figure (3) simulation results are displayed relative to a case where the robot starts from a double support phase: the right foot is moved backwards giving rise to a single support (on the left foot) phase and then the right foot is moved upwards kicking the ball. The target point to be used as reference for the GCoM is located at the center of the support polygon and it is assumed to have identically zero velocity. As expected, figure (3 (a)) shows that the error $r_t - r_{GCoM}$ is driven to zero by the action of the upper body joints (torso and arms). In figures (3 (b)-(c)) the values of the upper body joints $\theta_3, \theta_6, \theta_7$ (reported in figure 2) and their velocities are reported. Panel (d) shows a stick diagram of the robot movement in the sagittal plane. The GCoM tracking error is driven to zero by the action of arms and torso joints. At last in figure (4) simulation results are displayed without upper body joints control, namely the upper body joints are kept still in their initial values, the same used in the previous cases. As expected the x coordinate of GCoM leaves the support polygon resulting in the loss of stability (i.e. the robot falls down).

The robot used for the experimental validation is shown in figure (2). It is a Robovie-MS made by Vstone [23]. The robot has 17 degrees of freedom (DOFs): 5 in each leg, 3 in each arm and one in the head. It is 28 cm tall and has a total weight of about 860g. It has one 2 axis acceleration sensor and 17 joint angle sensors. The servos control board is composed by an H8 CPU at 20 MHz, a 56KByte FLASH-ROM memory, a 4KByte RAM and a 128KByte External-EEPROM. Experimental results relative to the implementation of the proposed control law are reported in figure (5). Notice that, as the joints are actuated by position servo motors, the control law (5) has been integrated in order to compute position references for the upper body joints. Given the limited communication bandwidth with the joint position servo controllers, during the experimental tests the position commands were updated at very low frequency (approximately 1Hz). In particular, the experimental results reported in figure (5) refer to the same

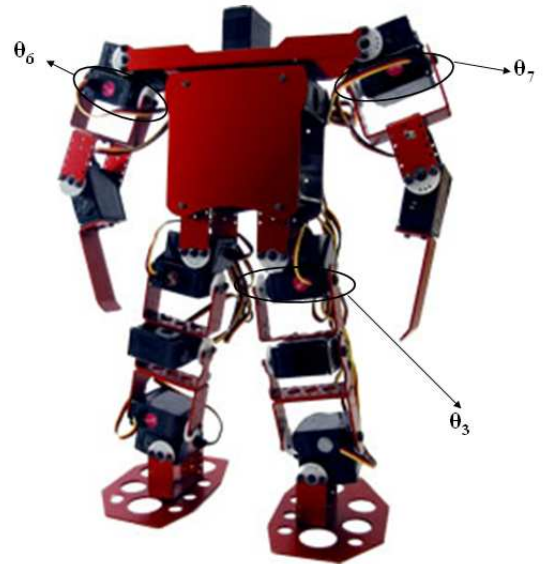


Fig. 2. Robovie-MS

situation of the simulations. The destabilizing x and y motion of the GCoM is automatically compensated by the upper body joints controlled by the proposed law.

In figure (6) we reported the same experiment of the figure (5) without upper body joints control and as expected the robot falls down after kicking the ball.

V. CONCLUSION

A method to control the upper body joints of a humanoid robot in order to stabilize it, has been presented. This method allows to decouple the gait generation issue from the stabilization one. The proposed solution is particularly suited for small size, low cost humanoid systems having limited computational power. Although due to HW constraints the experimental validation was possible only at rather low control update frequencies (approximately 1Hz), extensive trials have shown that leg motions that would have caused the robot to fall in case the upper body joints were kept still did *not* cause the robot to fall when the upper body joints were controlled according to the presented strategy. Simulations performed at higher update frequencies and higher link velocities confirm the effectiveness of the presented solution.

ACKNOWLEDGEMENTS

The anonymous reviewers are kindly acknowledged for their useful comments and suggestions.

REFERENCES

- [1] Honda (Inc), www.world.honda.com/ASIMO
- [2] Sony (Global), www.sony.net/SonyInfo/QRIO/
- [3] PINO The Humanoid, <http://www.symbio.jst.go.jp/%7Eyamasaki/>
- [4] RoboCup Official Site, <http://www.robocup.org/>
- [5] T. Tsuji and K. Ohnishi, "A control of biped robot which applies inverted pendulum mode with virtual supporting point", *AMC 2002*, Maribor, Slovenia, 2002.

- [6] M. Srinivasan and A. Ruina, "Computer optimization of a minimal biped model discovers walking and running", *Nature Letters to Editor*, 11 Sept. 2005.
- [7] A. Goswami, B. Espiau and A. Keramane, "Limit Cycles in a Passive Compass Gait Biped and Passivity-Mimicking Control Laws", *Autonomous Robots*, Vol. 4, pp. 273-286, 1997.
- [8] S. Kajita, F. Kanehiro, K. Kaneko, K. Fujiwara, K. Harada, K. Yokoi and H. Hirukawa, "Biped Walking Pattern Generation by using Preview Control of Zero-Moment Point", in Proc. of the *2003 IEEE/RSJ International Conference on Robotics and Automation*, Taipei, Taiwan, 2003.
- [9] R. Kurazume, T. Hasegawa and K. Yoneda, "The Sway Compensation Trajectory for a Biped Robot", in Proc. of the *2003 IEEE International Conference on Robotics and Automation*, Taipei, Taiwan, 2003.
- [10] Hun-ok Lim, Y. Yamamoto and A. Takanishi, "Control to realize human-like walking of a biped humanoid robot", in Proc. of *IEEE International Conference on Systems, Man, and Cybernetics*, 2000, 8-11 Oct. 2000, pp. 3271 - 3276 vol. 5.
- [11] A. Hoffman, M. Popovic, S. Massaquoi and H. Herr, "A sliding controller for bipedal balancing using integrated movement of contact and noncontact limbs", in Proc. of the *IEEE/RSJ IROS 2004 International Conference on Intelligent Robots and System*, (Sendai, Japan), 2004.
- [12] M. Vukobratović and D. Juricic, "Contribution to the synthesis of biped gait", *IEEE Trans. Bio-Medical Engineering*, Vol. 16, No. 1, pp. 1-6, 1969.
- [13] M. Vukobratović and B. Borovac, "Zero-Moment Point - Thirty five years of its life", *International Journal of Humanoid Robotics*, Vol. 1, No. 1, pp. 157-173, 2004.
- [14] A. Goswami, "Postural Stability of Biped Robots and the Foot-Rotation Indicator (FRI) Point", *The International Journal of Robotic Research*, Vol. 18, No. 6, pp. 523-533, 1999.
- [15] RoboCupSoccer Humanoid League Rules and Setup for the 2006 competition in Bremen, Germany, <http://www.humanoidsoccer.org/rules.html>
- [16] P. Kulvanit and others. "Team KMUTT: Team Description Paper", *RoboCup 2006 - Humanoid League Team Description Paper*.
- [17] S. Behnke and others. "NimbRo KidSize 2006 Team Description", *RoboCup 2006 - Humanoid League Team Description Paper*.
- [18] P. Kong Yue and others. "Robo-Erectus: KidSize and TeenSize Soccer-Playing Humanoid Robots", *RoboCup 2006 - Humanoid League Team Description Paper*.
- [19] N. M. Mayer and others. "JEAP Team Description", *RoboCup 2006 - Humanoid League Team Description Paper*.
- [20] Kagaku (Co. Ltd), www.kondo-robot.com
- [21] J. Baltes, S. McCann and J. Anderson. "Humanoid Robots: Abarenbou and DaoDan", *RoboCup 2006 - Humanoid League Team Description Paper*.
- [22] T. Röfer and others. "BreDoBrothers Team Description for RoboCup 2006", *RoboCup 2006 - Humanoid League Team Description Paper*.
- [23] Vstone (Co. Ltd), www.vstone.co.jp
- [24] T. Guseo and others, "Artisti Humanoid Team for RoboCup 2006", *RoboCup 2006 - Humanoid League Team Description Paper*.
- [25] N. Yamato and others, "VISION NEXTA: Fully autonomous humanoid robot", *RoboCup 2006 - Humanoid League Team Description Paper*.
- [26] Robotis Inc., Bioloid Robot Construction Kit, Korea.
- [27] M. Hild, M. Jünger and M. Spranger, "Humanoid Team Humboldt Team Description 2006", *RoboCup 2006 - Humanoid League Team Description Paper*.
- [28] A. Manni, A. di Noi and G. Indiveri, "A control architecture for dynamically stable gaits of small size humanoid robots", in Proc. of the *8th International IFAC Symposium on Robot Control SYROCO '06*, September 6 - 8, Bologna (Italy) 2006.
- [29] Y. Guan, E. S. Neo, and K. Yokoi, "Stepping Over Obstacles With Humanoid Robots", *IEEE Transactions on Robotics*, Vol. 22, No. 5, October 2006, pp. 958 - 973.
- [30] O. Khatib, L. Sentis, J. Park and J. Warren, "Whole-Body Dynamic Behavior And Control Of Human-Like Robots", *International Journal of Humanoid Robotics*, Vol. 1, No. 1, 2004, pp. 29 - 43.
- [31] L. Sciavicco and B. Siciliano, "Modelling and Control of Robot Manipulators", *Springer*, Berlin, 2000.
- [32] P. I. Corke, "A Robotics Toolbox for MATLAB", *IEEE Robotics and Automation Magazine* Vol 3, No. 1, 2004, pp. 24-32.

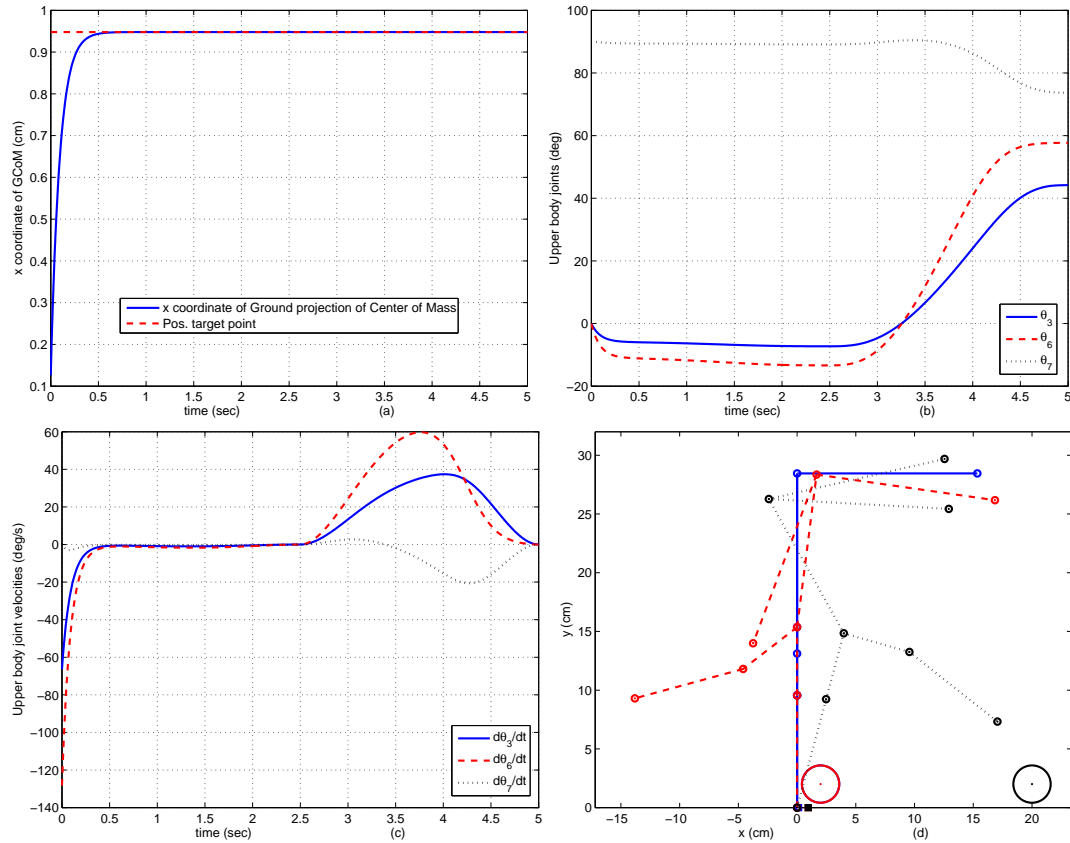


Fig. 3. Simulation 1: (a) position of the x coordinate of GCoM (solid line) and position of target point (dashed line); (b) θ_3 , θ_6 , θ_7 position, (c) θ_3 , θ_6 , θ_7 velocity, (e) stick diagram of start (solid line), middle (dashed line) and final (dotted line) configuration and position of the center of the support polygon (* (hidden under \square)) and the position of the center of mass (\square) in the sagittal plane

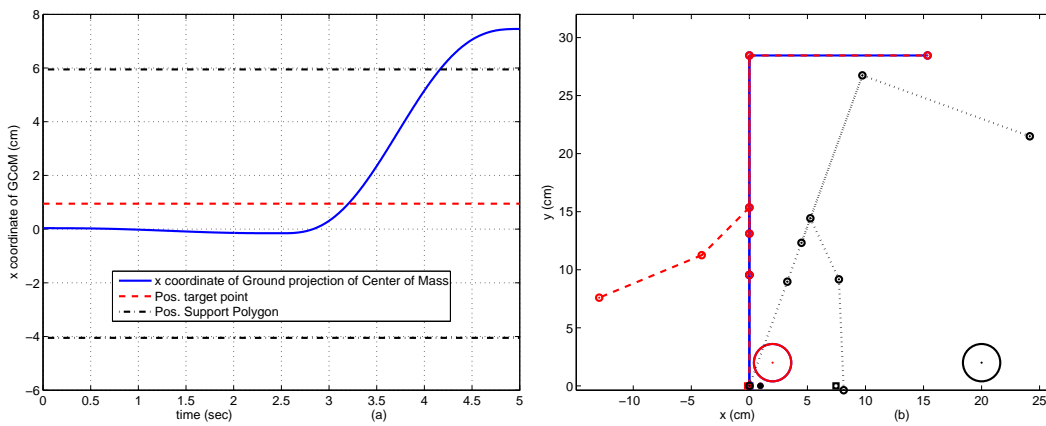


Fig. 4. Simulation 3: (a) position of the x coordinate of GCoM (solid line) and position of target point (dashed line) and position of support polygon (dash-dot line); (b) stick diagram of start (solid line), middle (dashed line) and final (dotted line) configuration and position of the center of the support polygon (*) and the position of the center of mass (\square)

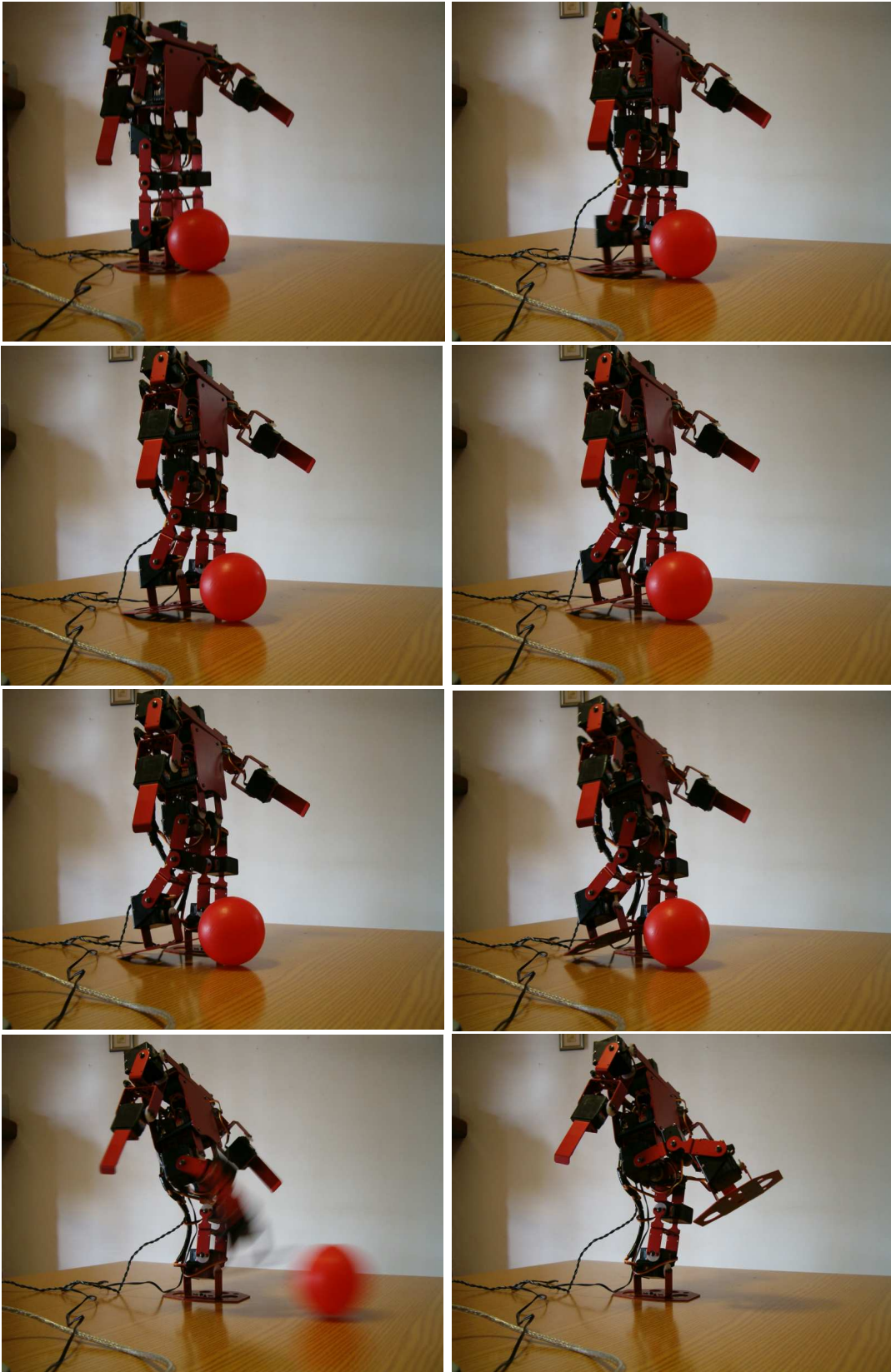


Fig. 5. Experimental results 1

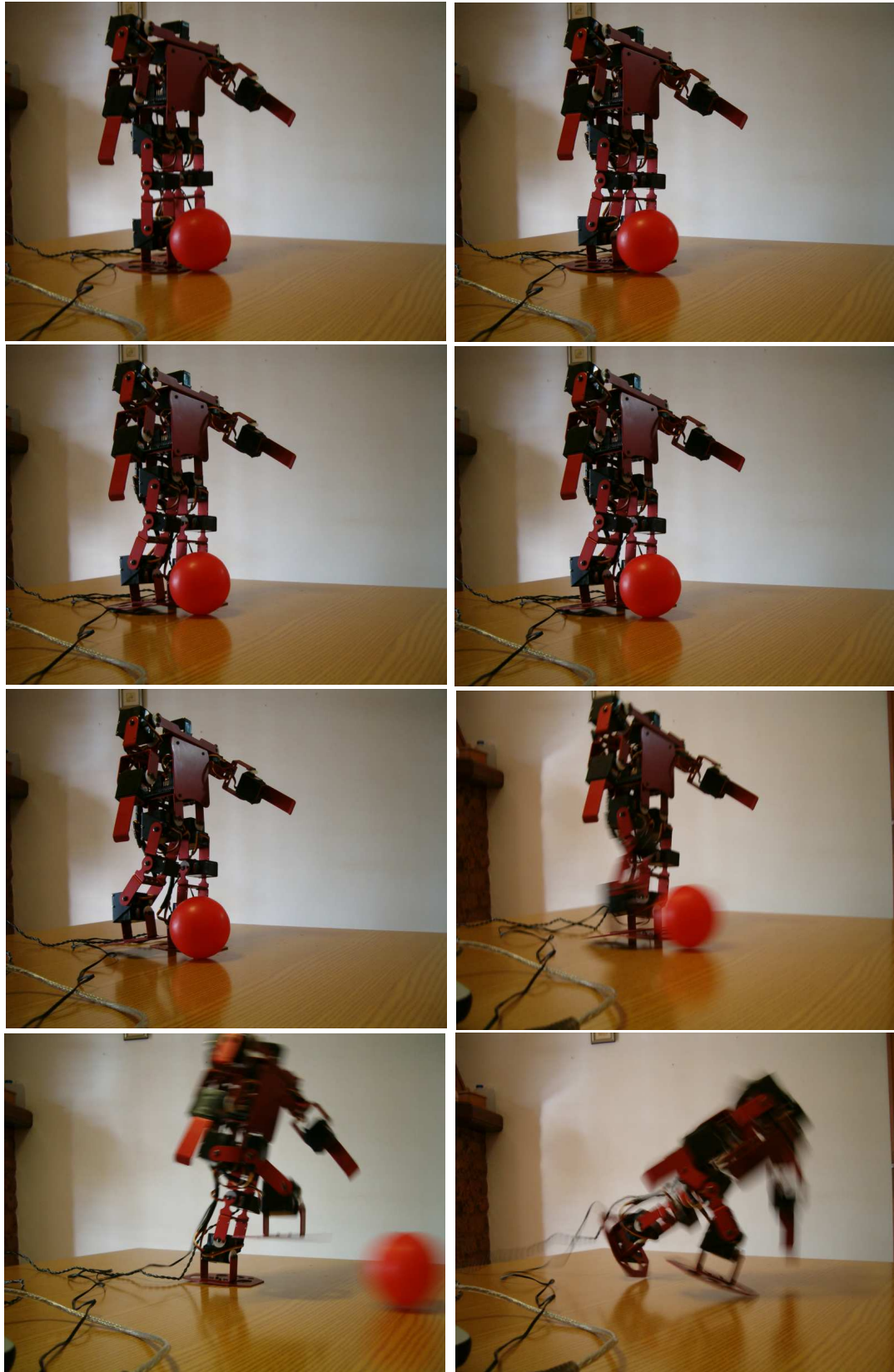


Fig. 6. Experimental results 2